

FIG. 3. Total polarization vs quench field: Total polarization is plotted for different incoming hydrogen atom velocities at varying quench fields. Velocities shown here are 1.0 a. u. (dot), 0.8 a. u. (plus sign), 0.6 a. u. (delta), and 0.4 a. u. (cross).

within 10% of that shown in Fig. 2(a). Both the exact numerical calculation and our approximation give results which are essentially indistinguishable at these velocities, slot widths, and field strengths. At higher velocities ($v \approx 10$ a. u.) and much narrower slot widths ($d \approx 0.01$ cm), the calculations diverge; however parameters in this range are not commonly used for cross section measurements and we do not consider them further.

In Fig. (3), a graph of the total polarization versus quench field is shown for various hydrogen atom velocities. The results indicate that the total polarization is very near the adiabatic value over the indicated ranges.

Thus we find that the adiabatic value for the total polarization may be used with less than 10% error for most experimental arrangements. Further, the determining factor for the value of the total polarization is the time to enter the electric field relative to the period associated with the fine structure splitting, not the Lamb splitting. If the entry time is larger than the fine-structure period, then the total polarization will be near its adiabatic value. Oscillations indicative of impulsive entry will appear in the instantaneous polarization when the entry time is less than or nearly equal to the Lamb period. If the entry time is larger than the Lamb period then, of course, there are no oscillations since this is clearly adiabatic. If the time to enter the field is less than or nearly equal to the fine-structure period, then an experimental measurement or a calculation such as that outlined in Sec. II C must be performed.

However, for most experimental arrangements used to measure H(2S) cross sections, the time to enter the field is sufficiently greater than the fine-structure period that the adiabatic value of the polarization can be used with less than 10% error.

¹W. R. Ott, W. E. Kauppila, and W. L. Fite, Phys. Rev. A **1**, 1089 (1970).

²D. H. Crandall and D. H. Jaecks (unpublished).

³W. R. Smythe, *Static and Dynamic Electricity*, 2nd ed. (McGraw-Hill, New York, 1950).

⁴H. A. Bethe and E. E. Salpeter, *Quantum Mechanics of One- and Two-Electron Atoms* (Springer-Verlag, Berlin, 1957).

⁵G. Lüders, Z. Naturforsch. **5a**, 608 (1950).

Discrepancy between Theory and Experiment for the Compton Profile of Molecular Hydrogen

Richard Edwin Brown and Vedene H. Smith, Jr.

Department of Chemistry, Queen's University, Kingston, Ontario, Canada

(Received 13 August 1971)

The Compton profile of the ground state of molecular hydrogen is calculated using the Liu 39-configuration-interaction (CI) wave function to confirm the experimental results of Eisenberger. This is in contrast to previous theoretical results obtained with the Hartree-Fock and Das-Wahl CI wave functions. The merits of these wave functions and also the best-overlap wave function are discussed.

INTRODUCTION AND METHOD

Compton x-ray scattering offers a useful and promising approach to the study of the electron momentum distribution (EMD) in atoms and molecules.

It is a particularly useful method for illustrating bonding and correlation effects. Dumond^{1,2} proposed and initially utilized this approach, and recent literature documents well the growing interest in Compton x-ray scattering.³⁻⁸

The profile of the Compton shifted line is the experimental result which allows direct comparison between theory and experiment. Although it is normally a difficult quantity to calculate, the impulse approximation (IPA)³ results in considerable simplifications for molecules containing only atoms of small nuclear charge. This approximation assumes that the binding energy of the electron is insignificant when compared to the energy imparted to it by the scattering x ray. With the IPA, the Compton profile assumes the following form for an isotropic system:

$$J(q) = \frac{1}{2} \int_{-\infty}^{\infty} [I_0(p)/p] dp, \quad (1)$$

where q equals the projection of the initial electron momentum p on the scattering vector of the x ray. $I_0(p)$ is the radial momentum distribution. It is usually evaluated from the wave function in momentum space which was either determined directly there or transformed from position space. It is more convenient to use the following prescription suggested and developed by Benesch and Smith.⁸ Thus, we have

$$I_0(p) = \int_0^\pi \sin\theta d\theta \int_0^{2\pi} d\phi p^2 \rho(\vec{p}|\vec{p}), \quad (2)$$

$$\rho(\vec{p}|\vec{p}') = (2\pi)^{-3} \int e^{-i\vec{p}\cdot\vec{r} + i\vec{p}'\cdot\vec{r}'} \gamma(\vec{r}|\vec{r}') d\vec{r} d\vec{r}'. \quad (3)$$

$\rho(\vec{p}|\vec{p}')$ is the Fourier transform of the one-electron density matrix $\gamma(\vec{r}|\vec{r}')$, which is defined as⁹

$$\begin{aligned} \gamma(\vec{r}_1|\vec{r}_1') &= N \int \psi(X_1, X_2, \dots, X_N) \psi^*(X_1', X_2', \dots, X_N') \\ &\quad \times ds_1 dX_2, \dots, dX_N, \end{aligned} \quad (4a)$$

$$\gamma(\vec{r}_1|\vec{r}_1') = \sum \lambda_k \chi_k(\vec{r}_1) \chi_k^*(\vec{r}_1'). \quad (4b)$$

The coordinate X_i denotes the combined space and spin coordinates of the i th electron, (\vec{r}_i, s_i) . In Eq. (4a), all space coordinates except \vec{r}_1 and \vec{r}_1' and all spin coordinates for each electron are set equal and the designated integration completed. The $\chi_k(\vec{r})$ are called the natural orbitals (NO), and the λ_k are the occupation numbers of the respective NO. Note that $J(0) = \frac{1}{2} \langle p^{-1} \rangle$ and that the traces of both $\gamma(\vec{r}|\vec{r}')$ and $\rho(\vec{p}|\vec{p}')$ equal N , the number of electrons.

The configuration-interaction (CI) wave function used here is that reported by Liu¹⁰ which gives an energy of -1.17363 hartree as compared to an experimental energy of -1.1744 hartree. This accounts for better than 98% of the correlation energy. Liu furnished the function in natural form such that

$$\Psi(1, 2) = \sum \lambda_k^{1/2} \chi_k(\vec{r}_1) \chi_k(\vec{r}_2) (\alpha\beta - \beta\alpha) / \sqrt{2}, \quad (5)$$

where with 19 σ , 12 π , and 8 δ NO, there was a total

TABLE I. Comparison of theoretical and experimental Compton profiles for $H_2(X^1\Sigma_g^+)$ at internuclear separation of 1.4 a.u.^a

q	H+H ^b	H ₂ -expt. ^c	Liu SCF	Das-Wahl		
				MC SCF ^b	Liu CI	Liu BO
0.0	1.698	1.513	1.553	1.573	1.529	1.540
0.1	1.648	1.475	1.516	1.532	1.493	1.505
0.2	1.509	1.378	1.412	1.416	1.393	1.403
0.3	1.311	1.240	1.258	1.249	1.245	1.253
0.4	1.088	1.065	1.077	1.060	1.069	1.075
0.5	0.869	0.887	0.890	0.871	0.888	0.891
0.6	0.675	0.712	0.715	0.699	0.717	0.718
0.7	0.513	0.561	0.562	0.551	0.566	0.565
0.8	0.385	0.435	0.433	0.429	0.440	0.437
0.9	0.286	0.334	0.330	0.330	0.337	0.334
1.0	0.212	0.255	0.250	0.253	0.257	0.253
1.2	0.117	0.150	0.141	0.147	0.147	0.143
1.4	0.065	0.089	0.079	0.085	0.084	0.081
1.6	0.038	0.051	0.045	0.049	0.049	0.046
1.8	0.022	0.030	0.026	0.029	0.029	0.027
2.0	0.014	0.015	0.015	0.017	0.017	0.016
KE =	1.000	1.174	1.126	1.157	1.174	1.142
$E_{total} =$...	-1.174 ^d	-1.134	-1.170	-1.174	...

^aAll values reported here are in a.u. with 1 hartree = 27.211 eV, 1 bohr = 0.52917 Å, and $\hbar = m = e = 1$, where m and e are the electronic mass and charge, respectively.

^bOur calculations for the two hydrogen atoms and the Das-Wahl wave function disagree by ± 0.001 a.u. with Eisenberger's results as reported by Eisenberger (Ref. 13).

^cEisenberger (Ref. 4) reported that the experimental errors are $\pm 0.7\%$ at $q=0.0$, $\pm 1\%$ at $q=0.6$, $\pm 3\%$ at $q=1.2$, and $\pm 10\%$ at $q=1.8$.

^dThe experimental energy of $H_2(X^1\Sigma_g^+) = -1.1744$ hartree.

of 39 natural configurations. Liu also reported a Hartree-Fock Self-Consistent-field (HF-SCF) function which gave an energy of -1.13360 hartree and was also used here. For a two-electron system, the first natural determinant of Eq. (5), i.e., $\chi_1(\vec{r}_1)\chi_1(\vec{r}_2)(\alpha\beta - \beta\alpha)/\sqrt{2}$, is both the best overlap (BO) determinant and the best density (BD) determinant¹¹ to the parent wave function. This simple function includes the "non-pure effects" correlation¹² to the electronic density, and its merits in representing the EMD are also discussed here. tion¹² to the electronic density, and its merits in representing the EMD are also discussed here.

RESULTS

In Table I are presented the Compton profile for two hydrogen atoms,¹³ the Das-Wahl Multiconfiguration-Self-Consistent-field (MC-SCF) function,¹⁴ the experimental results of Eisenberger,⁴ and the Liu SCF, CI, and BO functions.¹⁰ The Compton profiles for small and large values of q are plotted in Figs. 1 and 2 respectively.

In order to test the validity of the IPA, Eisenberger⁴ has recently made very precise measurements of

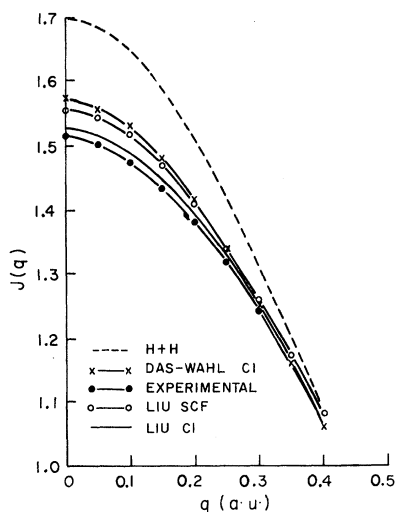


FIG. 1. Compton profiles of $H_2(X^1\Sigma_g^+)$ for $q \leq 0.40$ a.u. The curves for H+H, the Das-Wahl function, and the experimental results were originally reported by Eisenberger (Ref. 4).

the Compton profile for helium and molecular hydrogen. Eisenberger's experimental results for He agreed very well with the theoretical calculations of Henneker. The theoretical profiles for both the Hartree-Fock and correlated functions lay well within the experimental errors of the He profiles reported by Eisenberger. However for $H_2(X^1\Sigma_g^+)$, there was a substantial discrepancy between theory and experiment. Henneker¹³ reported profiles calculated from the HF SCF wave function of Cade¹⁵ and the MC SCF function of Das and Wahl.¹⁴ The HF SCF profile was well outside the experimental error bounds while the correlated profile was even more so for the smaller values of q . Thus for He, calculations within the IPA agreed well with experiment while the opposite was true for H_2 . We felt that the Das-Wahl result was particularly suspect since it gave a $J(0) = \frac{1}{2} \langle p^{-1} \rangle$ value larger than the HF SCF result (see Table I). Since $\langle p^2 \rangle_\psi > \langle p^2 \rangle_{\text{HF}}$ for a correlated wave function ψ which obeys the virial theorem,¹⁶ and $\langle p^0 \rangle_\psi = \langle p^0 \rangle_{\text{HF}}$, one would normally expect that $\langle p^{-1} \rangle_\psi < \langle p^{-1} \rangle_{\text{HF}}$.¹⁷ Thus as more correlation was included in a wave function, the electronic density with low momentum would decrease and that with high momentum would increase. The Das-Wahl function gave the opposite result for the electronic density with small momentum. Although the Das-Wahl function does not satisfy the virial theorem, scaling it did not remove the discrepancy and only lowered $J(0)$ slightly (~ 0.0004 a. u.). Thus we felt that the Compton profile of a more accurate wave function was in order to test the validity of the experimental results as

well as the IPA.

The plots for small q demonstrate that the Liu CI function gives the best profile with a substantial reduction of the low-momentum components over both the SCF and Das-Wahl functions. For the larger momentum components, the Liu CI function gives the expected increase in the profile, and for $q > 1.2$ a. u. the Liu and Das-Wahl CI functions agree very well. Actually with respect to the Liu CI function, the Das-Wahl function gives a poor momentum distribution only for $q < 1.0$ a. u. It is somewhat disturbing that the Liu function, with 98% of the correlation energy, still gives an error of 1% for $J(0)$, which is slightly greater than the experimental error of 0.7%. However for the values of $J(q)$ for larger momentum components, the Liu CI results lie well inside the experimental-error bounds. Expected corrections to the theoretical profile with more correlation should bring the theory into even better agreement with experiment.

The BO function gave a profile very similar to that of the Liu CI function and a $J(0)$ value about half way between the CI and SCF values. The main deficiency of the BO function is that χ_1 is a σ function and lacks the high-momentum components of a π or δ NO which give $J(q)$ a broader profile. However, the BO profile is better than the SCF profile since the Liu BO function is the determinant which best fits the Liu CI density.

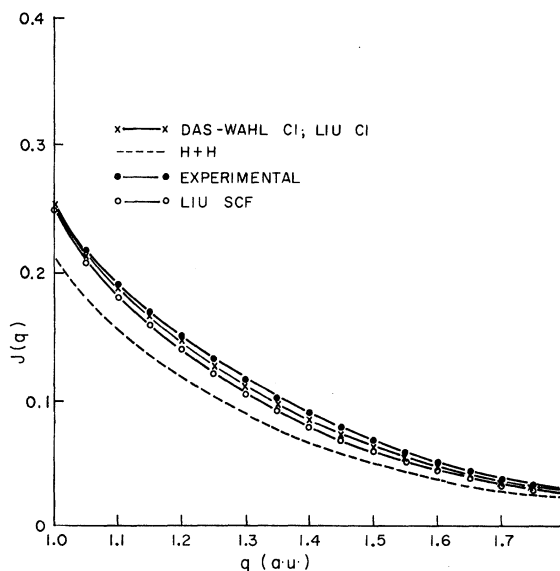


FIG. 2. Compton profiles of $H_2(X^1\Sigma_g^+)$ for $1.0 \leq q \leq 1.8$ a. u. The curves for H+H, the Das-Wahl function, and the experimental results were originally reported by Eisenberger (Ref. 4). For these values of q , the Das-Wahl and Liu CI values could not be distinguished graphically.

ACKNOWLEDGMENTS

We wish to thank Bowen Liu for providing us with

- ¹J. W. H. Dumond, *Phys. Rev.* **33**, B643 (1929).
²J. W. H. Dumond and H. A. Kirkpatrick, *Phys. Rev.* **52**, 419 (1937).
³P. Eisenberger and P. M. Platzman, *Phys. Rev. A* **2**, 415 (1970).
⁴P. Eisenberger, *Phys. Rev. A* **2**, 1678 (1970).
⁵R. J. Weiss, *X-Ray Determination of Electron Distributions* (Wiley, New York, 1966).
⁶R. J. Weiss, *Acta Cryst.* **A25**, 248 (1969).
⁷W. C. Phillips and R. J. Weiss, *Phys. Rev.* **171**, 790 (1968).
⁸Vedene H. Smith, Jr. and R. Benesch, in *Proceedings of the International Symposium on the Physics of One and Two Electron Atoms*, Munich, 1968 (unpublished); R. Benesch and Vedene H. Smith, Jr., *Chem. Phys. Letters* **5**, 601 (1970); *Intern. J. Quantum Chem.* **4**, 131 (1971); this issue, *Phys. Rev. A* **5**, 114 (1970).

the details of his H₂ wave function and Professor Werner Brandt for helpful comments on the manuscript.

- ⁹P. O. Löwdin, *Phys. Rev.* **97**, 1474 (1955).
¹⁰B. Liu (unpublished).
¹¹W. Kutzelnigg and V. H. Smith, Jr., *J. Chem. Phys.* **42**, 896 (1964).
¹²R. E. Brown, S. Larsson, and Vedene H. Smith, Jr., *Phys. Rev. A* **2**, 593 (1970).
¹³W. Hennecker, quoted in Ref. 4.
¹⁴G. Das and A. C. Wahl, *J. Chem. Phys.* **44**, 87 (1966).
¹⁵P. Cade, quoted in Ref. 4.
¹⁶For a diatomic molecule at the equilibrium distance, the virial theorem states that $\langle E \rangle = -\langle T \rangle = \frac{1}{2} \langle V \rangle$. By definition of correlation, the energy of a correlated wave function is less than the HFSCF energy.
¹⁷This is not rigorously true, as the Das-Wahl wave function demonstrates. However, previous work with very accurate wave functions have always given this intuitive result (Ref. 8).

Molecular Parameters of OH Free Radical*

Masataska Mizushima

Department of Physics and Astrophysics, University of Colorado, Boulder, Colorado 80302

(Received 16 July 1971)

Theoretical formulas with higher-order perturbation terms are given for the rotational levels of ²Π states, and are applied to the OH free radical. By analyzing existing data values of several molecular parameters including the rotational constant *B*, the spin-orbit coupling constant *A* and Λ-doublet constants *α* and *β* are obtained for some vibrational states. The magnetic *g* factors are discussed and analyzed. A recent experiment on laser magnetic resonance (LMR) is also discussed.

I. INTRODUCTION

Diatomic molecules, including diatomic free radicals such as OH, are more complicated than atoms but still simple enough to allow detailed theoretical treatment. The rotational and vibrational levels of a diatomic molecule are particularly simple, because the Born-Oppenheimer approximation,¹ namely, the semirigid body model, is known to be applicable. Many data are carefully analyzed according to this model.^{2,3}

Most stable diatomic molecules are in the ¹Σ electronic state, but there are some which have finite electronic angular momenta in their ground states. The oxygen molecule has electron spin angular momentum *S* = 1 in its electronic ground states, which makes each rotational level a triplet. The triplet separations in this case are measured and analyzed, and some molecular parameters for that molecule are obtained.⁴⁻⁶ The OH free radical, our present subject, is another typical case. Its electronic ground state is ²Π; namely, the electronic orbital

angular momentum around the molecular axis is + 1 or - 1, and the electronic spin angular momentum *S* is $\frac{1}{2}$.

Because of the spin-orbit coupling, the spin can orient itself either in parallel or antiparallel direction to the orbital angular momentum, producing the splitting into the Π_{3/2} and Π_{1/2} states. Since the coupled electronic angular momenta can be either in parallel or antiparallel direction to the molecular axis, which we call the *z* axis, each of these two states is doubly degenerate. The degeneracy is slightly removed due to the end-over-end rotation, and gives the so-called Λ doublet. The theory of rotational states of a ²Π molecules was given by Van Vleck⁷ and by Mulliken and Christy.⁸

The uv spectrum of OH was measured and analyzed by Johnston, Dawson, and Walker many years ago.^{9,10} Much more extensive and accurate measurement was done by Dieke and Crosswhite,¹¹ who reported many rotational and vibrational levels of the ground ²Π states. Transitions within each Λ doublet can be observed in microwave spectroscopy.